wall width is properly selected, the fundamental resonant frequency of inner triangular PIFA can be coupled with the resonance that is introduced by the V-slot, and consequently a wide-band operation is obtained in the higher frequency band. A large operating bandwidth of 36% has been demonstrated. In addition, the radiation patterns across the entire operating bands are also measured; the antenna gain is about 4 and 4.3 dBi for the lower and higher frequency bands, respectively.

References

[1] K. L. Wong, M. C. Pan, and W. H. Hsu, "Single-feed dual-frequency triangular microstrip antenna with a V-shaped slot," *Microwave Opt. Technol. Lett.*, vol. 20, pp. 133–134, Jan. 1999.

[2] T. Huynh and K. F. Lee, "Single-layer single-patch wideband microstrip antenna," *Electron. Lett.*, vol. 31, pp. 1310–1312, Aug. 1995.

[3] K. M. Luk, K. F. Lee, and W. L. Tam, "Circular U-slot patch with dielectric superstrate," *Electron. Lett.*, vol. 33, pp. 1001–1002, Jun. 1997.

[4] P. Salonen, M. Keskilammi, and M. Kivikoski, "Single-feed dual-band planar inverted-F antenna with U-shaped slot," *IEEE Trans. Antennas Propag.*, vol. 48, pp. 1262–1264, Aug. 2000.

[5] ——, "Dual-band and wide-band PIFA with U- and meanderline-shaped slots," in *IEEE Trans. Antennas Propag. Symp. Dig.*, vol. 2, Jul. 2001, pp. 8–13.

[6] D. Nashaat, H. A. Elsadek, and H. Ghali, "A wideband compact shorted rectangular microstrip patch antenna with U-shaped slot," in *IEEE Trans. Antennas Propagat. Symp. Dig.*, vol. 2, Jun. 2003, pp. 22–27.

[7] Y. X. Guo, K. M. Luk, K. F. Lee, and R. Chair, "A quarter-wave U-shaped patch antenna with two unequal arms for wideband and dual-frequency operation," *IEEE Trans. Antennas Propag.*, vol. 50, pp. 1082–1087, Aug. 2002.

[8] K. Ogawa and T. Uwano, "A diversity antenna for very small 800-MHz band portable telephones," *IEEE Trans. Antennas Propag.*, vol. 42, pp. 1342–1345, Sep. 1994.

[9] Y. Yoshimura, "A microstripline slot antenna," *IEEE Trans. Microwave Theory Tech.*, vol. MTT-20, pp. 760–762, Nov. 1972.

On Wave Boundary Elements for Radiation and Scattering Problems With Piecewise Constant Impedance

Emmanuel Perrey-Debain, Jon Trevelyan, and Peter Bettess

***Abstract*—Discrete methods of numerical analysis have been used successfully for decades for the solution of problems involving wave diffraction, etc. However, these methods, including the finite element and boundary element methods, can require a prohibitively large number of elements as the wavelength becomes progressively shorter. In this paper, a new type of interpolation for the wave field is described in which the usual conventional shape functions are modified by the inclusion of a set of plane waves propagating in multiple directions. Including such a plane wave basis in a boundary element formulation is found in this paper to be highly successful. Results are shown for a variety of scattering/radiating problems from convex and nonconvex obstacles on which are prescribed piecewise constant Robin conditions. Notable results include a conclusion that, using this new formulation, only approximately three degrees of freedom per wavelength are required.**

***Index Terms*—Boundary integral equation, Helmholtz equation, impedance, plane waves, wave scattering.**

Manuscript received November 5, 2003; revised July 22, 2004. This work was supported by the EPSRC, under Grant GR/N09879.

E. Perrey-Debain is with the Department of Mathematics, University of Manchester, Manchester M13 9PL, U.K. (e-mail: emmanuel@maths.man.ac.uk).

J. Trevelyan and P. Bettess are with the School of Engineering, University of Durham, Durham DH1 3LE, U.K.

Digital Object Identifier 10.1109/TAP.2004.841274

I. Introduction

It is well known that the use of discrete (frequency domain) numerical methods for the solution of the Helmholtz equation is limited to problems in which the wavelength under consideration is not small in comparison with the domain size. The limitation arises because conventional elements, based on polynomial shape functions, can reliably capture only a limited portion of the sinusoidal waveform. A commonly quoted rule of thumb requires eight to ten nodes per full wavelength. It can quickly be seen that problems involving large domains and short waves may require impractically large computational resources. This applies to both finite element and boundary element simulations.

Following earlier predictions of de La Bourdonnaye [1] and the partition of unity method introduced by Melenk and Babuška [2], it has been found that drastic progress can be made by including the essential wave character of the wave field in the element formulation. To be more precise, we assume that the solution can be written as a finite sum of terms like $a_i(\boldsymbol{r})\exp(i\kappa\boldsymbol{\xi}_i\cdot\boldsymbol{r})$ where the point $\boldsymbol{r}$ belongs either to the propagative domain Ω in a finite element volume discretization scheme (see, for example, [3] and [4]) or its boundary $\gamma=\partial\Omega$ in a boundary element discretization scheme arising from integral equations. Functions $a_i(\boldsymbol{r})$ are "slowly" varying functions compactly supported and vectors $\boldsymbol{\xi}_i$, which define the wave directions, are of unit amplitude. In [5], we give details of the implementation of the method in a boundary element context and investigate its accuracy and numerical characteristics, including the condition number of the resulting system matrix. Numerical scattering results on simple geometries showed that this new formulation can provide extremely accurate results at a relatively low cost (up to eight digits accuracy with only four variables per wavelength) [6], [7] and allows the frequency range to be extended by a factor of three to four for bidimensional problems.

In this paper, we deal with more complicated situations in which part of the scatterer can be radiating and/or absorbing as well. We show, through various numerical examples, that the "wave boundary elements" method remains very efficient and should have, we hope, a significant impact on the modeling of shortwave problems in many different fields.

II. Formulation

We consider a two-dimensional obstacle of general shape with smooth boundary in an infinite propagative medium impinged upon by a time-harmonic wave $\Phi^{\rm inc}$. By using the direct formulation via the Green second identity, the 2-D Helmholtz equation is reformulated into a boundary integral equation on the boundary γ as follows (the usual $e^{-i\omega t}$ time-dependence is adopted):

$$\frac{1}{2}\Phi(\boldsymbol{r})+\int_\gamma \nabla G(\boldsymbol{r},\boldsymbol{r}')\cdot\boldsymbol{n}\Phi(\boldsymbol{r}')\,d\gamma(\boldsymbol{r}') - \int_\gamma G(\boldsymbol{r},\boldsymbol{r}')\nabla\Phi(\boldsymbol{r}')\cdot\boldsymbol{n}\,d\gamma(\boldsymbol{r}')=\Phi^{\rm inc}(\boldsymbol{r}) \quad (1)$$

where $\boldsymbol{n}$ is the normal unit vector at point $\boldsymbol{r}'$ directed into the obstacle, G is the free-space Green function $G(\boldsymbol{r},\boldsymbol{r}')=(i/4)\,H_0(\kappa|\boldsymbol{r}-\boldsymbol{r}'|)$, where H_0 is the Hankel function of the first kind of order zero, and $i=\sqrt{-1}$. κ is the wavenumber given by $\kappa=2\pi/\lambda$, where λ is the wavelength. Along the boundary are imposed the following general impedance boundary conditions of the form:

$$\nabla\Phi\cdot\boldsymbol{n}=i\alpha\Phi+\beta \quad \text{on } \gamma \quad (2)$$

where α,β are two complex-valued functions defined on the boundary. In the acoustic case, Φ is the velocity potential and α is called the surface admittance, which is absorbing if $\Re e(\alpha) \geq 0$. In the electromagnetic case, the Dirichlet problem (respectively, Neumann) corresponds to TM (respectively, TE) electromagnetic scattering.

We consider obstacles whose boundaries admit the parameterization

$$\gamma : \boldsymbol{r} = \boldsymbol{r}(s), \quad s \in [0, 2\pi] \tag{3}$$

where s is the curvilinear abscissa. We assume throughout that α and β are piecewise constant such that

$$\alpha(s) = \alpha_j, \quad s \in]s_j, s_{j+1}[\tag{4}$$

$$\beta(s) = \beta_j, \quad s \in]s_j, s_{j+1}[\tag{5}$$

for some $0 = s_1 < s_2 < \cdots < s_n < s_{n+1} = 2\pi$. On each subdomain $\boldsymbol{r}(s), s \in]s_j, s_{j+1}[$, we define the basis function Φ_j^q as a propagative plane wave of unit direction $\boldsymbol{\xi}_q$ modulated by the conventional quadratic shape functions

$$\Phi_j^q(\boldsymbol{r}) = \frac{1}{2}\left(\phi_{j,q}^1 \ \phi_{j,q}^2 \ \phi_{j,q}^3\right)\begin{pmatrix} t(t-1) \\ 2(1-t^2) \\ t(t+1) \end{pmatrix} \exp(i\kappa\boldsymbol{\xi}_q \cdot \boldsymbol{r}) \tag{6}$$

where $\{\phi_{j,q}^e\}_{e=1,2,3}$ represent the basis function coefficients. The parameter t is defined over [−1,1] and varies linearly with the curvilinear abscissa s as $t = (2s - s_j - s_{j+1})/(s_{j+1} - s_j)$.

The solution space is constructed by introducing Q plane waves propagating in various directions evenly distributed over the unit circle $\boldsymbol{\xi}_q = (\cos(q2\pi/Q), \sin(q2\pi/Q))$, so that we can write the solution of (1) in the compact form

$$\Phi(\boldsymbol{r}) = \sum_{j=1}^{n}\sum_{q=1}^{Q}\Phi_j^q(\boldsymbol{r}), \quad \boldsymbol{r} \in \gamma. \tag{7}$$

The boundary element $\boldsymbol{r}(s)_{s_j<s<s_{j+1}}$ is expected to span over many wavelengths and is named "wave boundary element." The integral formulation (1) is enforced by point-matching at points regularly distributed over the boundary line. Irregular frequency effects are avoided using Schenck's method [9]. For more details concerning implementation and integration schemes, one can refer to [5]. In the next section, we assess the efficiency of the method for both convex and nonconvex obstacles.

III. Results

Our first numerical tests concern radiating and scattering by the unit circle $\boldsymbol{r}(\theta) = (\cos\theta, \sin\theta)$, for which analytic solutions can be obtained via Fourier series. For the sake of simplicity, we restrict ourselves to a regular subdivision $s_j = \theta_j = (j-1)2\pi/n$ and we consider an incident plane wave propagating in the direction $\boldsymbol{d}$

$$\Phi^{\text{inc}}(\boldsymbol{r}) = \exp(i\kappa\boldsymbol{d} \cdot \boldsymbol{r}). \tag{8}$$

Let us assume that $\boldsymbol{d} = (1, 0)$. In the exterior region ($r \geq 1$), the analytical solution can be expanded in polar coordinates as

$$\Phi^{\text{ana}}(r,\theta) = \sum_m (A_m H_m(\kappa r) + i^m J_m(\kappa r))e^{im\theta} \tag{9}$$

where H_m and J_m are, respectively, Hankel and Bessel functions of the first kind of order m. Now, let $\hat{\alpha}_m$ and $\hat{\beta}_m$ be the Fourier components of, respectively, α and β. We call v the nth root of unity $v = e^{i2\pi/n}$. Straighforward calculations then yield

$$\hat{\alpha}_0 = \frac{1}{n}\sum_{j=1}^{n}\alpha_j \tag{10}$$

$$\hat{\alpha}_m = \frac{i(1-v^m)}{2\pi m}\sum_{j=1}^{n}\alpha_j v^{-jm}, \quad m \neq 0 \tag{11}$$

and similarly for $\hat{\beta}_m$. Injecting (9) in (2) yields the following (infinite) system for the unknown coefficients A_m:

$$\sum_p (i\hat{\alpha}_{m-p}H_p(\kappa) + \kappa H_p'(\kappa)\delta_{mp})A_p = -\sum_p \hat{\alpha}_{m-p}i^{p+1}J_p(\kappa) - i^m\kappa J_m'(\kappa) - \hat{\beta}_m \tag{12}$$

where δ is the Kronecker symbol and the prime denotes differentiation with respect to the argument. For numerical reasons, it is strongly advised to consider the variable $B_p = H_p(\kappa)A_p$ so that the impedance matrix coefficients

$$Z_{mp} = i\hat{\alpha}_{m-p} + \kappa\frac{H_p'(\kappa)}{H_p(\kappa)}\delta_{mp}$$

remain bounded. When $p \gg \kappa$, asymptotic forms for Hankel functions are used [10].

Obviously, the series (9) is convergent only in the least square sense and relatively "poor" convergence is expected at the discontinuity points θ_j [this is even more the case for components $\hat{\alpha}_m, \hat{\beta}_m$ whose magnitude decreases only as $\mathcal{O}(m^{-1})$]. Nevertheless, this is not a major issue here since in our applications we are interested in "engineering accuracy" (say, in the range 0.1–1%).

Performances of the method are conveniently summarized in Table I. The first two rows are concerned with the radiation from the unit circle of 50λ width. The error is measured in the L_2-norm as

$$\varepsilon_2 = \left(\frac{\int_\gamma |\Phi(\boldsymbol{r}) - \Phi^{\text{ana}}(\boldsymbol{r})|^2\, d\gamma(\boldsymbol{r})}{\int_\gamma |\Phi^{\text{ana}}(\boldsymbol{r})|^2\, d\gamma(\boldsymbol{r})}\right)^{1/2}. \tag{13}$$

We can note that these values are overestimated since the analytical solution is not accurate. It could be useful to develop a better formula than the "slowly" converging Fourier series (9). In this regard, one can refer to [11] for a rigourous numerical treatment for acoustic scattering in half-plane by a surface of piecewise constant impedance. On the last column is shown the average discretization level (i.e., the number of degrees of freedom per wavelength). The corresponding graphs of the magnitude $|\Phi|$ along the boundary line are plotted in Figs. 2 and 3. The agreement is excellent and differences between curves are not discernible. In example (ii), one can see the presence (or not) of the absorbers.

Test (iii) shows the efficiency of the wave boundary elements when dealing with a pure scattering problem. Indeed, 2.8 variables per wavelength are sufficient to get three to four digit accuracy results. One can see in Fig. 4 some stationary waves occuring at the vicinity of the junctions s_j. These effects are absent when the impedance is constant on the surface of the obstacle.

In order to give a fair comparison with other methods, the scattering example (iii) has been tested with two other kinds of approximation schemes (see Table II). Note that in both formulations, the exact mapping (3) is considered so that errors are not influenced by the geometry description. When using the conventional quadratic shape functions, at least ten variables per wavelength are needed to get accuracy below 1%. Obviously, if one is only interested in the far-field pattern then

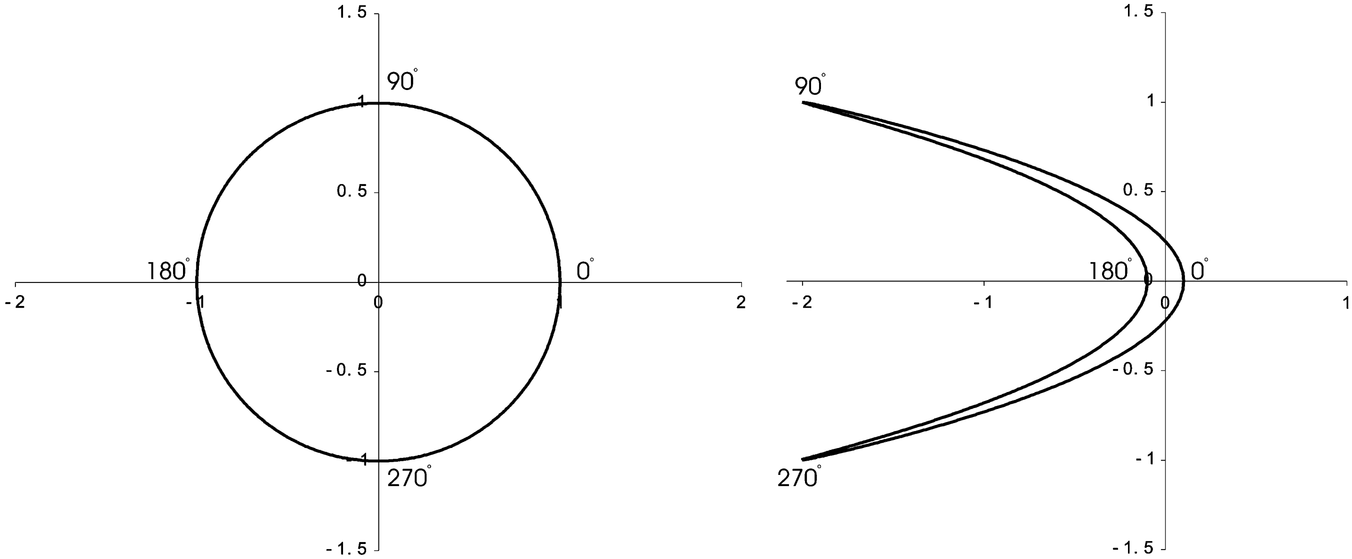

Fig. 1. Geometry of the obstacles considered in our calculations.

TABLE I
5 TESTED CONFIGURATIONS ($\lambda = 0.04$ AND $z = 1 + i$). (*) ZERO VALUES ARE NOT ON DISPLAY

	Obstacle	n	Q	$\boldsymbol{d}$	Boundary conditions (*)	ε_2	Disc. lev.
(i)	Circle	4	55	-	$\beta_1 = 100z$, $\beta_2 = 50z$, $\alpha_2 = 100\bar{z}$, $\alpha_4 = 10\bar{z}$	0.3 %	2.8
(ii)	Circle	8	30	-	$\beta_{1,3,5,7} = 100z$, $\alpha_{4,8} = 100\bar{z}$	0.4 %	3.0
(iii)	Circle	4	55	(1,0)	$\alpha_2 = 100\bar{z}$, $\alpha_4 = 10\bar{z}$	0.1 %	2.8
(iv)	Eq.(14)	4	90	(1,0)	$\alpha_{2,3} = 100\bar{z}$	< 0.1 %	3.0
(v)	Eq.(14)	4	90	(-1,0)	$\alpha_{2,3} = 100\bar{z}$	< 0.1 %	3.0

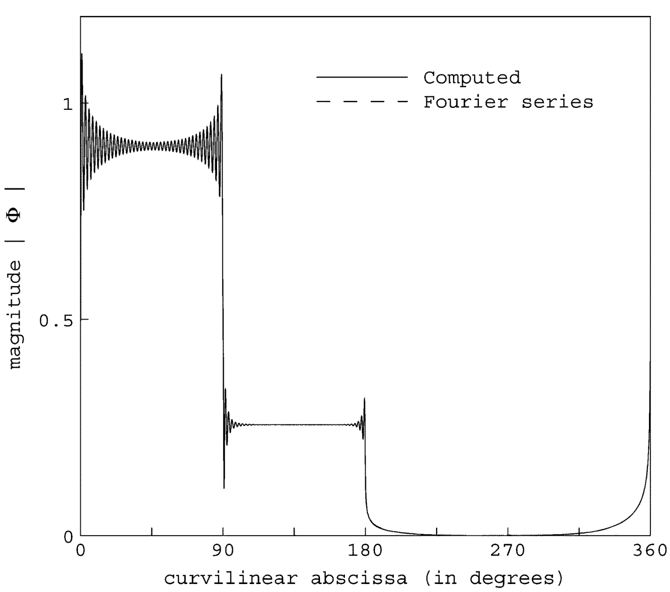

Fig. 2. Surface "current" magnitude $|\Phi|$ for test (i).

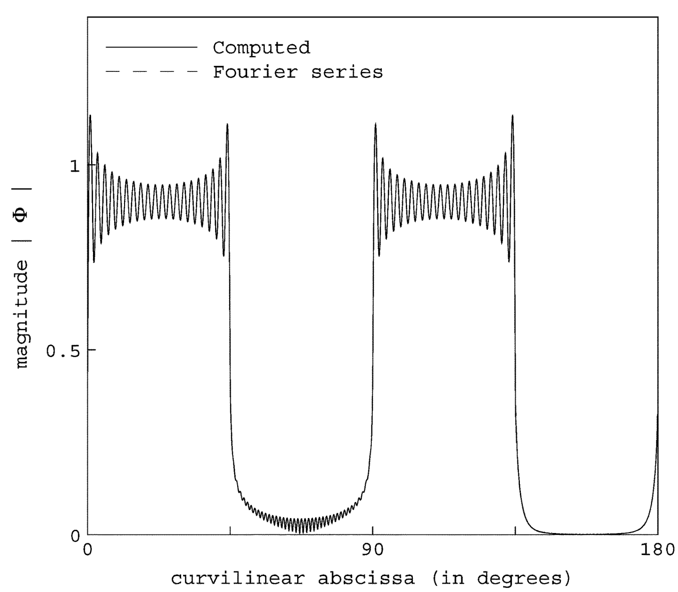

Fig. 3. Surface "current" magnitude $|\Phi|$ for test (ii).

five variables per wavelength could be sufficient. As clearly shown, the complexity can be reduced by a factor 2 if the reduced potential Φ/Φ^{inc} (instead of Φ) is taken as the unknown (see similar treatments in [8], [12], and [13] and recent developments of the method in [14]). When dealing with the specific case of the scattering by smooth *convex* nonradiating obstacles with constant surface admittance, this "reduced" formulation is known as stemming from asymptotic theory and leads to a $\mathcal{O}(\kappa^{1/3})$ complexity [8], [7]. In the current case, the performances offered by this latter are significantly affected due to discontinuity effects and our "wave boundary element" method remains competitive.

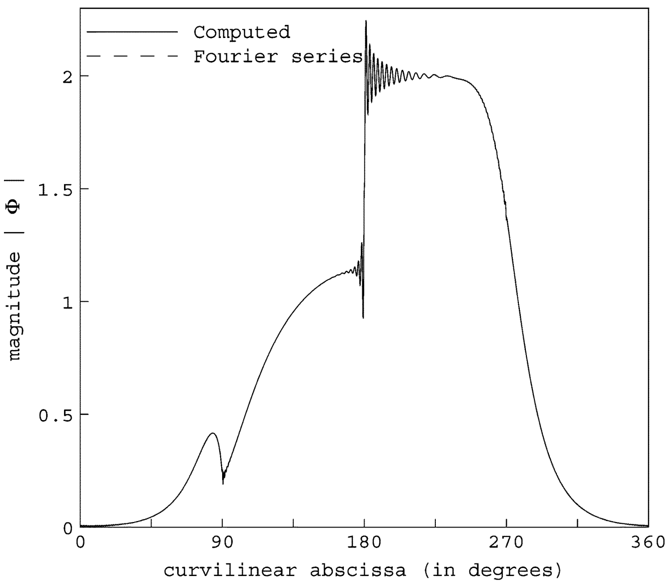

Fig. 4. Surface "current" magnitude $|\Phi|$ for test (iii).

TABLE II
COMPARISON WITH OTHER KINDS OF APPROXIMATION SCHEME FOR TEST (iii)

Approx. scheme	ε_2	Disc. lev.
	5.6 %	5.1
Quadratic approx. for Φ	0.7 %	10.2
	0.2 %	15.3
	2.8 %	2.6
Quadratic approx. for $\Phi/\Phi^{\rm inc}$	0.8 %	5.1
	0.3 %	7.6

In test (iv), we increase the difficulty by considering a nonconvex reflector whose shape is illustrated in Fig. 1 and given by the following parameterization:

$$\boldsymbol{r}(s) = ([\cos s + 10\cos 2s - 10]/10, \sin s), \quad s \in [0, 2\pi]. \quad (14)$$

The illuminated zone $s \in [\pi/2, 3\pi/2]$ is covered with an absorbing layer $\alpha_2 = \alpha_3 = 100(1-i)$. In the shadow zone, the admittance is set to zero. Three calculations have been carried out with, respectively, 90, 100, and 120 directions. On Fig. 5 are plotted the magnitude of the potential and differences between curves are hardly noticeable. The global L_2-error between these three sets of results is estimated to be below 0.1%. One can observe standing waves of very small magnitude in the "silent" zone $-10^\circ \leq s(\deg) \leq 10^\circ$.

Test (v) deals with the same obstacle and an incident wave travelling in the opposite direction $\boldsymbol{d} = (-1, 0)$. Here again, results obtained are of very good quality even in the shadow region, and the stability of our method is clearly shown in these examples.

IV. CONCLUSION

This paper has presented some tests illustrating the numerical performance of the wave boundary elements method for the solution of the Helmholtz equation. The potential is expressed in nodal form as the amplitude of some artificial plane waves travelling in various directions.

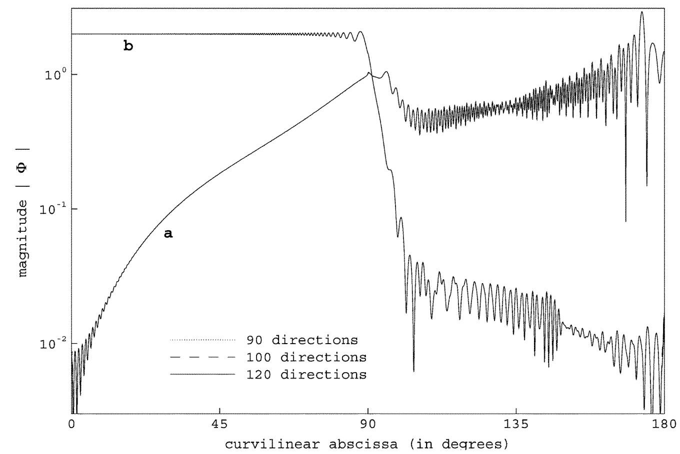

Fig. 5. Surface "current" magnitude $|\Phi|$ for test (iv) [curve labeled $\mathbf{a}$ with $\boldsymbol{d} = (1, 0)$] and test (v) [curve labeled $\mathbf{b}$ with $\boldsymbol{d} = (-1, 0)$].

The modulation of this plane wave basis, provided by the polynomial shape functions, gives the boundary solution. The method is applicable for convex and nonconvex scatterers on the surface of which are imposed general Robin conditions. In practical terms, the method is expected to provide three to four digit accuracy of results with a relatively low discretization level of three variables per wavelength.

REFERENCES

[1] A. de La Bourdonnaye, "Convergence of the approximation of wave functions by oscillatory functions in the high frequency limit," *C. R. Acad. Sci. Paris*, ser. I, vol. 318, pp. 765–768, 1994.
[2] J. M. Melenk and I. Babuška, "The partition of unity method," *Int. J. Numer. Meth. Eng.*, vol. 40, pp. 727–758, 1997.
[3] O. Laghrouche, P. Bettess, and R. J. Astley, "Modeling of short diffraction wave problems using approximating system of plane waves," *Int. J. Numer. Meth. Eng.*, vol. 54, pp. 1501–1533, 2002.
[4] P. Ortiz and E. Sanchez, "An improved partition of unity finite element model for diffraction problems," *Int. J. Numer. Meth. Eng.*, vol. 50, pp. 2727–2740, 2000.
[5] E. Perrey-Debain, J. Trevelyan, and P. Bettess, "Plane wave interpolation in direct collocation boundary element method for radiation and wave scattering: Numerical aspects and applications," *J. Sound Vib.*, vol. 261, no. 5, pp. 839–858, 2003.
[6] ——, "Using wave boundary elements in BEM for high frequency scattering," in *Proc. 3rd U.K. Conf. Boundary Integral Methods*, Brighton, U.K., Sep. 2001, pp. 119–128.
[7] ——, "Numerical aspects of single wave basis boundary elements for acoustic scattering," in *Proc. 4th U.K. Conf. Boundary Integral Methods*, Salford, U.K., Sep. 2003, pp. 77–86.
[8] T. N. Abboud, J.-C. Nédélec, and B. Zhou, "Méthodes des équations intégrales pour les hautes fréquences," *C. R. Acad. Sci. Paris*, ser. I, vol. 318, pp. 165–170, 1994.
[9] H. A. Schenck, "Improved integral formulation for acoustic radiation problems," *J. Acoust. Soc. Amer.*, vol. 44, pp. 41–58, 1968.
[10] *Handbook of Mathematical Functions*, 10th ed., National Bureau of Standards, U.S. Government Printing Office, Washington, DC, 1972.
[11] S. N. Chandler-Wilde, S. Langdon, and L. Ritter, "A high wavenumber boundary element method for an acoustic scattering problem," *Phil. Trans. Roy. Soc. London A*, vol. 362, pp. 647–671, 2004.
[12] K. R. Aberegg and A. F. Peterson, "Application of the integral equation-asymptotic phase method to dimensional scattering," *IEEE Trans. Antennas Propag.*, vol. 43, no. 5, pp. 534–537, May, 1995.
[13] J. M. James, "A contribution to scattering calculation for small wavelengths—The high frequency panel method," *IEEE Trans. Antennas Propag.*, vol. 38, no. 10, pp. 1625–1630, Oct. 1990.
[14] O. P. Bruno, C. A. Geuzaine, J. A. Monro, and F. Reitich, "Prescribed error tolerances within fixed computational times for scattering problems of arbitrarily high frequency: The convex case," *Phil. Trans. Roy. Soc. London A*, vol. 362, pp. 629–645, 2004.